



Assessing the strength of directed influences among neural signals using renormalized partial directed coherence

Björn Schelter^{a,b,c,*}, Jens Timmer^{a,b,c,d}, Michael Eichler^e

^a FDM, Freiburg Center for Data Analysis and Modeling, University of Freiburg, Eckerstr. 1, 79104 Freiburg, Germany

^b Physics Department, University of Freiburg, Hermann-Herder-Str. 3, 79104 Freiburg, Germany

^c Bernstein Center for Computational Neuroscience, University of Freiburg, Freiburg, Germany

^d Freiburg Institute for Advanced Studies, University of Freiburg, Albertstr. 19, 79104 Freiburg, Germany

^e Department of Quantitative Economics, University of Maastricht, P.O. Box 616, 6200 MD Maastricht, The Netherlands

ARTICLE INFO

Article history:

Received 11 October 2008

Received in revised form 9 January 2009

Accepted 10 January 2009

Keywords:

Partial directed coherence

Granger-causality

Multivariate time series

Graphical models

Renormalization

ABSTRACT

Partial directed coherence is a powerful tool used to analyze interdependencies in multivariate systems based on vector autoregressive modeling. This frequency domain measure for Granger-causality is designed such that it is normalized to [0,1]. This normalization induces several pitfalls for the interpretability of the ordinary partial directed coherence, which will be discussed in some detail in this paper. In order to avoid these pitfalls, we introduce renormalized partial directed coherence and calculate confidence intervals and significance levels. The performance of this novel concept is illustrated by application to model systems and to electroencephalography and electromyography data from a patient suffering from Parkinsonian tremor.

© 2009 Elsevier B.V. All rights reserved.

1. Introduction

When analyzing networks in neuroscience an inverse problem has to be faced. From measured time series conclusions about the underlying systems are desired. Of particular interest is the analysis of interrelations between the processes. Understanding such interrelations enables a deeper understanding of the functioning or dysfunctioning of networks in neuroscience (Grosse et al., 2002; Hellwig et al., 2000, 2001, 2003; Hesse et al., 2003; Tass et al., 1998; Volkman et al., 1996).

Several time series analysis techniques have been suggested to analyze interactions between processes (e.g. Dahlhaus et al., 1997; Eichler et al., 2003; Rosenblum and Pikovsky, 2001; Smirnov and Bezruchko, 2003; Timmer et al., 1998). In this manuscript we concentrate on a parametric technique that has been introduced as being capable of analyzing not only multivariate networks in neuroscience and to infer interrelations therein but also to allow conclusions about causal dependencies. The so-called partial directed coherence (Baccala and Sameshima, 2001; Sameshima and Baccala, 1999) is based on the concept of Granger-causality (Granger, 1969), which is based on the common sense idea that

causes precede their effects in time and is formulated in terms of predictability.

We mention though that in the literature other techniques have been suggested to infer the causal interaction structure in multivariate systems. The directed transfer function (DTF), which provides the direction of information flow, but cannot distinguish direct interactions is widely applied in neuroscience research (Kamiński and Blinowska, 1991; Kamiński et al., 2001). Another technique in the time domain, which is also capable in differentiating direct and indirect interactions is the so-called Granger-causality index (Hesse et al., 2003). The advantages and disadvantages of several techniques have been discussed in the literature (see for instance Winterhalder et al., 2005; Eichler, 2006).

To infer Granger-causality by partial directed coherence, a vector autoregressive model of appropriate order p (VAR[p]) is usually fitted to the data. Fourier transformation of the coefficients of the vector autoregressive processes yields the partial directed coherence. Its statistical properties have recently been examined (Schelter et al., 2006). In particular, a significance level for testing non-zero partial directed coherences at fixed frequencies has been suggested. Even though there is now a strict mathematical procedure to decide statistical significance of partial directed coherence values, some desired interpretations of partial directed coherence are impossible or at least difficult. For instance, it is impossible to compare partial directed coherence values, that is, a higher partial directed coherence value does not necessarily indicate a higher coupling between the processes. The reason for this can be

* Corresponding author at: FDM, Freiburg Center for Data Analysis and Modeling, University of Freiburg, Eckerstr. 1, 79104 Freiburg, Germany. Tel.: +49 761 203 7711; fax: +49 761 203 7700.

E-mail address: schelter@fdm.uni-freiburg.de (B. Schelter).

found in the normalization procedure. Thereby, the partial directed coherence value does relate to the coupling strength and to the number and strength of all influenced processes.

To overcome this limitation we suggest a new normalization strategy for partial directed coherence. We show that the statistics for this renormalized partial directed coherence are based on a χ^2 -distribution with two degrees of freedom. This leads to a significance level as well as confidence intervals for partial directed coherence that allow inference of statistical significance and comparison of two partial directed coherence values.

In Section 2, partial directed coherence is summarized with the original normalization. The significance level is briefly presented to illustrate the problems with interpretability of the ordinary partial directed coherence. Furthermore, we introduce the renormalized partial directed coherence and derive its statistical properties. In Section 3, the performance of the new statistic is evaluated by a Monte Carlo study based on a linear stochastic model and two non-linear systems, including one in the chaotic regime. Finally, an application to electroencephalographic (EEG) and electromyographic (EMG) recordings from a patient suffering from Parkinsonian tremor is presented in Section 4.

2. Partial directed coherence

In the following, the concepts of Granger-causality and partial directed coherence (PDC) are briefly introduced and the main problems related to the interpretation of PDC and its estimates are discussed. This discussion will lead to a modified version of the PDC, the renormalized partial directed coherence.

2.1. Definition and statistical properties

Let $\mathbf{x} = (\mathbf{x}(t))_{t \in \mathbb{Z}}$ with $\mathbf{x}(t) = (x_1(t), \dots, x_n(t))'$ be a stationary n -dimensional time series with mean zero. Then a vector autoregressive model of order p , abbreviated VAR[p], for \mathbf{x} is given by

$$\mathbf{x}(t) = \sum_{r=1}^p \mathbf{a}(r) \mathbf{x}(t-r) + \boldsymbol{\varepsilon}(t), \quad (1)$$

where $\mathbf{a}(r)$ are the $n \times n$ coefficient matrices of the model and $\boldsymbol{\varepsilon}(t)$ is a multivariate Gaussian white noise process. The covariance matrix of the noise process is denoted by $\boldsymbol{\Sigma}$. The model is stationary if the coefficients satisfy the condition:

$$\det(I - \mathbf{a}(1)z - \dots - \mathbf{a}(p)z^p) \neq 0, \quad (2)$$

for all $z \in \mathbb{C}$ such that $|z| \leq 1$ (e.g. Lütkepohl, 1993), where I denotes the $n \times n$ identity matrix. In the following, it is assumed that the condition in Eq. (2) holds.

In this model, the coefficients $\mathbf{a}_{ij}(r)$ describe how the present values of x_i depend linearly on the past values of the components x_j . More precisely, the process x_j is said to Granger-cause another process x_i with respect to the full process \mathbf{x} if in the autoregressive representation in Eq. (1) the entries $\mathbf{a}_{ij}(r)$, $r = 1, \dots, p$, are not all zero or, in other words, if linear prediction of $x_i(t+1)$ based on the past and present values of all variables but x_j can be improved by adding the past and present values of x_j . The concept of Granger-causality originates from econometrics and has been introduced by Granger (1969).

We note that the vector autoregressive modeling approach allows only the description of linear relationships among the variables and hence, strictly speaking, relates to linear Granger-causality. In the sequel, we will use “Granger-causality” in this restricted meaning.

In order to provide a frequency domain measure for Granger-causality, Baccala and Sameshima (2001) introduced the concept of partial directed coherence. This measure has been derived from

a factorization of the partial spectral coherence and is based on the Fourier transform of the coefficient series:

$$\mathbf{A}(\omega) = I - \sum_{r=1}^p \mathbf{a}(r) e^{-i\omega r}. \quad (3)$$

More precisely, the partial directed coherence from x_j to x_i is defined as

$$|\pi_{i \leftarrow j}(\omega)| = \frac{|\mathbf{A}_{ij}(\omega)|}{\sqrt{\sum_k |\mathbf{A}_{kj}(\omega)|^2}}. \quad (4)$$

Because of condition (2) the denominator is strictly positive, which guarantees that the partial directed coherence is well defined. Furthermore, the PDC $|\pi_{i \leftarrow j}(\omega)|$ takes values between 0 and 1 and vanishes for all frequencies ω if and only if the coefficients $\mathbf{a}_{ij}(r)$ are zero for all $r = 1, \dots, p$. Thus, the PDC $|\pi_{i \leftarrow j}(\omega)|$ provides a measure for the direct linear influence of x_j on x_i at frequency ω . More precisely, it compares the linear influence of process x_j on the process x_i at the frequency ω with the influence of x_j on the other variables, that is, partial directed coherence ranks the interaction strengths with respect to a given signal source.

The interpretation of causality related to frequency is of course challenging. However, there is a rigorous meaning what causality at a certain frequency indicated by a significant partial directed coherence refers to. It indicates that if the frequency content of the source signal at a certain frequency was raised, the corresponding frequency component of the Granger-causally influenced signal would change accordingly.

The partial directed coherence $|\pi_{i \leftarrow j}(\omega)|$ is estimated by fitting an n -dimensional VAR[p] model to the data and using Eqs. (3) and (4) with the parameter estimates $\hat{\mathbf{a}}_{ij}(k)$ substituted for the true coefficients $\mathbf{a}_{ij}(k)$. The statistical properties of the estimates of partial directed coherence $|\hat{\pi}_{i \leftarrow j}(\omega)|$ can be derived from those of the parameter estimates $\hat{\mathbf{a}}_{ij}(k)$ (Schelter et al., 2006). In particular, it has been shown that, if $|\mathbf{A}_{ij}(\omega)|^2 = 0$, the asymptotic distribution for N data points of

$$\frac{N}{C_{ij}(\omega)} |\hat{\mathbf{A}}_{ij}(\omega)|^2 \quad (5)$$

is that of a weighted average of two independent χ^2 -distributed random variables each with one degree of freedom. We mention that for $p = 1$ or $p \geq 2$ and $\omega = 0 \bmod \pi$ it was shown in Schelter et al. (2006) that the distribution is a χ^2 -distribution with one degree of freedom.

The denominator of Eq. (5) is given by

$$C_{ij}(\omega) = \boldsymbol{\Sigma}_{ii} \left[\sum_{k,l=1}^p \mathbf{H}_{ij}(k, l) (\cos(k\omega) \cos(l\omega) + \sin(k\omega) \sin(l\omega)) \right], \quad (6)$$

with $\mathbf{H}_{ij}(k, l)$ being the entries of the inverse $\mathbf{H} = \mathbf{R}^{-1}$ of the covariance matrix \mathbf{R} of the VAR process \mathbf{x} . The critical values of this distribution are bounded by the corresponding critical values of a χ^2 -distribution with one degree of freedom. It follows that the null hypothesis of $|\hat{\pi}_{i \leftarrow j}(\omega)| = 0$ can be rejected if the estimated PDC exceeds the value:

$$\left(\frac{\hat{C}_{ij}(\omega) \chi_{1, 1-\alpha}^2}{N \sum_k |\hat{\mathbf{A}}_{kj}(\omega)|^2} \right)^{1/2}, \quad (7)$$

where $\chi_{1, 1-\alpha}^2$ denotes the $1 - \alpha$ quantile of the χ^2 -distribution with one degree of freedom and $\hat{C}_{ij}(\omega)$ is an estimate of $C_{ij}(\omega)$ in Eq. (6). For details see Schelter et al. (2006).

2.2. Disadvantages of partial directed coherence

The pointwise significance level allows identifying those frequencies at which the PDC differs significantly from zero, which indicates the existence of a direct influence from the source to the target variable. More generally, one is interested in comparing the strength of directed relationships at different frequencies or between different pairs of variables. Such a quantitative interpretation of the PDC and its estimates, however, is hampered by a number of problems.

First, PDC measures the strength of influences relative to a given signal source. This seems counter-intuitive since the strength of coupling is not affected by the number of other series that are influenced by the source process. In particular, adding further variables that are influenced by the source variable decreases the PDC although the relationship between source and target process remains unchanged. This property prevents meaningful comparisons of influences between different source processes or even between different frequencies as the denominator in Eq. (4) varies over frequency. In contrast it is expected that the influence of the source on the target process is diminished by an increasing number of other processes that affect the target variable, which suggests to measure the strength relative to the target process. This leads to the alternative normalizing term:

$$\left(\sum_k |\hat{\mathbf{A}}_{ik}(\omega)|^2 \right)^{1/2}, \quad (8)$$

which may be derived from the factorization of the partial spectral coherence in the same way as the original normalization by [Baccala and Sameshima \(2001\)](#). Such a normalization with respect to the target process has been used by [Kamiński and Blinowska \(1991\)](#) in their definition of the directed transfer function. We note that either normalization may be favorable in some applications but not in others.

Second, PDC is not scale-invariant, that is, it depends on the units of measurement of the source and the target process. In particular, the PDC can take values arbitrarily close to either one or zero if the scale of the target variable is changed accordingly. This problem becomes important especially if the involved variables are not measured on a common scale; an example for such an application is provided in Section 4, where data from electroencephalography and electromyography are jointly analyzed for the discussion of tremor related interactions between the cortex and the periphery.

Third, when the PDC is estimated, further problems arise from the fact that the significance level in Eq. (7) depends on the frequency unlike, for instance, the significance level for the spectral coherence ([Bloomfield, 1976](#)). In particular, we find that the critical values compensate for the effects of normalization by $\sqrt{\sum_k |\hat{\mathbf{A}}_{ij}(\omega)|^2}$, that is, the significance of the PDC essentially depends on the absolute rather than the relative strength of the interaction. Although the pointwise significance level adapts correctly to the varying uncertainty in the estimates of the PDC, this behavior shows clearly the need for measures of confidence in order to be able to compare estimates at different frequencies. Without such measures, it remains open how to interpret large peaks that exceed the significance level only slightly and how to compare them with smaller peaks that are clearly above the threshold.

In summary, the discussion has shown that PDC as a measure of the relative strength of directed interactions does not allow conclusions on the absolute strength of coupling and is not suited for comparing the strength at different frequencies or between different pairs of variables. Moreover, the frequency dependence of the significance level shows that large values of the PDC are not necessarily more reliable than smaller values, which weakens the

interpretability of the PDC further. In the following, we show that these problems may be overcome by a different normalization.

2.3. A new definition of PDC: renormalized PDC

For the derivation of an alternative normalization, recall that the PDC is defined in terms of the Fourier transform $\mathbf{A}_{ij}(\omega)$ in Eq. (3). Since this quantity is complex-valued, it is convenient to consider the two-dimensional vector:

$$\mathbf{X}_{ij}(\omega) = \begin{pmatrix} \text{Re} & \mathbf{A}_{ij}(\omega) \\ \text{Im} & \mathbf{A}_{ij}(\omega) \end{pmatrix}, \quad (9)$$

with $\mathbf{X}_{ij}(\omega)' \mathbf{X}_{ij}(\omega) = |\mathbf{A}_{ij}(\omega)|^2$. The corresponding estimator $\hat{\mathbf{X}}_{ij}(\omega)$ with $\hat{\mathbf{A}}_{ij}(\omega)$ substituted for $\mathbf{A}_{ij}(\omega)$ is asymptotically normally distributed with mean $\mathbf{X}_{ij}(\omega)$ and covariance matrix $\mathbf{V}_{ij}(\omega)/N$, where

$$\mathbf{V}_{ij}(\omega) = \sum_{k,l=1}^p \mathbf{H}_{ij}(k, l) \Sigma_{ii} \begin{pmatrix} \cos(k\omega) \cos(l\omega) & \cos(k\omega) \sin(l\omega) \\ \sin(k\omega) \cos(l\omega) & \sin(k\omega) \sin(l\omega) \end{pmatrix}. \quad (10)$$

For $p \geq 2$ and $\omega \neq 0 \bmod \pi$, the matrix $\mathbf{V}_{ij}(\omega)$ is positive definite ([Schelter et al., 2006](#)), and it follows that, for large N , the quantity

$$N \hat{\lambda}_{ij}^{\circ}(\omega) = N \hat{\mathbf{X}}_{ij}(\omega)' \mathbf{V}_{ij}(\omega)^{-1} \hat{\mathbf{X}}_{ij}(\omega)$$

has approximately a noncentral χ^2 -distribution with two degrees of freedom and noncentrality parameter $N \lambda_{ij}(\omega)$, where

$$\lambda_{ij}(\omega) = \mathbf{X}_{ij}(\omega)' \mathbf{V}_{ij}(\omega)^{-1} \mathbf{X}_{ij}(\omega).$$

If $p = 1$ or $\omega = 0 \bmod \pi$, the matrix $\mathbf{V}_{ij}(\omega)$ has only rank one and thus is not invertible. However, similar arguments as in [Schelter et al. \(2006\)](#) show that in this case $N \hat{\lambda}_{ij}^{\circ}(\omega)$ with $\mathbf{V}_{ij}(\omega)^{-1}$ being a generalized inverse of $\mathbf{V}_{ij}(\omega)$ has approximately a noncentral χ^2 -distribution with one degree of freedom and noncentrality parameter $N \lambda_{ij}(\omega)$.

The parameter $\lambda_{ij}(\omega)$, which is nonnegative and equals zero if and only if $\mathbf{A}_{ij}(\omega) = 0$, determines how much $\mathbf{X}_{ij}(\omega)$ and thus $\mathbf{A}_{ij}(\omega)$ differ from zero. Consequently, it provides an alternative measure for the strength of the effect of the source process x_j on the target process x_i .

The most important consequence of the normalization by $\mathbf{V}_{ij}(\omega)$ is that the distribution of $\hat{\lambda}_{ij}^{\circ}(\omega)$ depends only on the parameter $\lambda_{ij}(\omega)$ and the sample size N . In particular, it follows that the α -significance level for $\hat{\lambda}_{ij}^{\circ}(\omega)$ is given by $\chi_{df, 1-\alpha}^2/N$ and thus is constant unlike in the case of the PDC. Here, $\chi_{df, 1-\alpha}^2$ denotes the $1 - \alpha$ quantile of the χ^2 -distribution with the corresponding degrees of freedom (2 or 1). More generally, confidence intervals for the parameter $\lambda_{ij}(\omega)$ can be computed; algorithms for computing confidence intervals for the noncentrality parameter of a noncentral χ^2 -distribution can be found, for instance, in [Kent and Hainsworth \(1995\)](#). We note that the properties of noncentral χ^2 -distributions (e.g. [Johnson et al., 1995](#)) imply that the end-points of such confidence intervals for $\lambda_{ij}(\omega)$ increase monotonically with $\hat{\lambda}_{ij}^{\circ}(\omega)$, that is, large values of the estimates are indeed likely to correspond to strong influences among the variables. Finally, we note that the parameter $\lambda_{ij}(\omega)$ is also scale invariant which can be shown by few evaluations.

With these properties, $\hat{\lambda}_{ij}^{\circ}(\omega)$ seems an “ideal” estimator for $\lambda_{ij}(\omega)$. However, it cannot be computed from data since it depends on the unknown covariance matrix $\mathbf{V}_{ij}(\omega)$. In practice, $\mathbf{V}_{ij}(\omega)$ needs to be estimated by substituting estimates $\hat{\mathbf{H}}$ and $\hat{\Sigma}$ for \mathbf{H} and Σ in Eq. (10). This leads to the alternative estimator:

$$\hat{\lambda}_{ij}(\omega) = \hat{\mathbf{X}}_{ij}(\omega)' \hat{\mathbf{V}}_{ij}(\omega)^{-1} \hat{\mathbf{X}}_{ij}(\omega).$$

It can be shown by Taylor expansion that under the null hypothesis of $\lambda_{ij}(\omega) = 0$ this statistic is still χ^2 -distributed with two respectively one degrees of freedom, that is, the α -significance level remains unchanged when $\hat{\lambda}_{ij}^{\circ}(\omega)$ is replaced by $\hat{\lambda}_{ij}(\omega)$. In contrast, the exact asymptotic distribution of the new estimator under the alternative is not known. Nevertheless, the simulations in the next section show that approximate confidence intervals can be obtained by applying the theoretical results obtained for the “ideal” estimator $\hat{\lambda}_{ij}^{\circ}(\omega)$ to the practical estimator $\hat{\lambda}_{ij}(\omega)$.

3. Simulations

In the first part of this section we demonstrate the performance of the proposed significance level for a vector autoregressive process. We shall see that the method even works well when the true model is overfitted. This robustness becomes particularly important when an unknown system is investigated since the correct order of the process is not known. In this first example that should serve as an illustrative example we assume that the asymptotic distribution of $\hat{\lambda}_{ij}(\omega)$ is identical to that of $\hat{\lambda}_{ij}^{\circ}(\omega)$. In a second example the performance of the renormalized partial directed coherence $\hat{\lambda}_{ij}(\omega)$ in combination with its confidence intervals and significance level is tested in a more rigorous manner. This analysis shows that for practical purposes the distributional properties of $\hat{\lambda}_{ij}^{\circ}(\omega)$ can be used for the evaluation of the estimator $\hat{\lambda}_{ij}(\omega)$. In a third example we show that renormalized partial directed coherence is not influenced by a certain strength of the signal source. In a fourth and fifth example, to further illustrate the wide-spread applicability of renormalized partial directed coherence we apply it to a system of coupled non-linear van-der-Pol oscillators and to a system of coupled Rössler oscillators in the chaotic regime. These non-linear systems are genuine examples where model-overfitting is inevitable as high model orders are required to model the non-linear behavior sufficiently well (Schelter et al., 2006).

3.1. Vector autoregressive process I

The five-dimensional VAR[3] process:

$$x_1(t) = 0.9x_1(t-1) + 0.3x_2(t-2) + \varepsilon_1(t), \quad (11)$$

$$x_2(t) = 1.3x_2(t-1) - 0.8x_2(t-2) + \varepsilon_2(t), \quad (12)$$

$$x_3(t) = 0.3x_1(t-2) + 0.6x_2(t-1) + \varepsilon_3(t), \quad (13)$$

$$x_4(t) = -0.7x_4(t-3) - 0.7x_1(t-3) + 0.3x_5(t-3) + \varepsilon_4(t), \quad (14)$$

$$x_5(t) = 1.0x_5(t-1) - 0.4x_5(t-2) + 0.3x_4(t-2) + \varepsilon_5(t), \quad (15)$$

serves as a first example for the performance of the renormalized partial directed coherence and the corresponding confidence intervals. Here, the ε_j are standard normally distributed random variables. In this example 3.000 data points have been simulated. For the fitted model system a VAR of order 50 was used, thus, a considerably overfitting of the true model which is of order 3. The following directed interactions are present, from process $x_1 \rightarrow x_3$, $x_1 \rightarrow x_4$, $x_2 \rightarrow x_1$, $x_2 \rightarrow x_3$, $x_4 \rightarrow x_5$, and $x_5 \rightarrow x_4$. This is guaranteed by non-zero coefficients in the model system.

In Fig. 1 the results for the renormalized partial directed coherence analysis are shown. The figure represents the renormalized partial directed coherence estimated from one single realization of the system. The results are sorted as a matrix, where in the i th row and the j th column the influence from process x_j onto process x_i is displayed. The gray areas are the confidence intervals. If the confidence interval is compatible with zero, the directed influence is not considered to be present. This is also indicated by the dashed horizontal line, which is the 5%-level of significance.

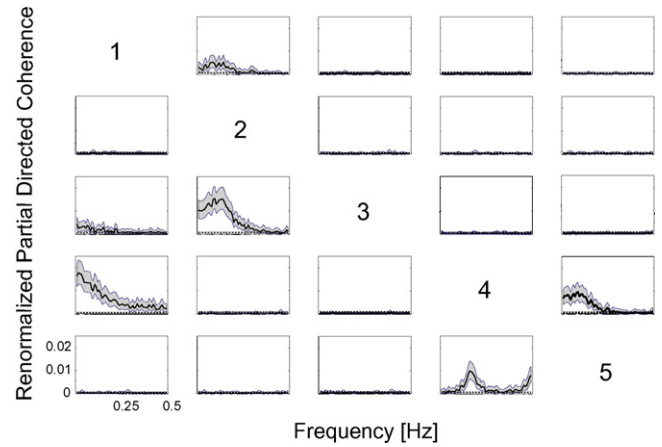


Fig. 1. Renormalized partial directed coherence (off-diagonal) for the example of the VAR[3] process. Results are sorted as a matrix, where in the i th row and the j th column the influence from process j onto process i is displayed. The solid lines are the renormalized partial directed coherence values and the corresponding 5%-confidence intervals are indicated by the gray areas. The dashed horizontal lines are the 5% significance levels. The simulated causal influences are reproduced correctly since only partial directed coherences $|\pi_{3 \leftarrow 1}|$, $|\pi_{4 \leftarrow 1}|$, $|\pi_{1 \leftarrow 2}|$, $|\pi_{3 \leftarrow 2}|$, $|\pi_{5 \leftarrow 4}|$, and $|\pi_{4 \leftarrow 5}|$ are significant. The influence from process $x_4 \rightarrow x_5$ and vice versa $x_5 \rightarrow x_4$ are of similar strength as the renormalized partial directed coherences take similar values. The interaction from process $x_2 \rightarrow x_3$ and $x_1 \rightarrow x_4$ are stronger than the $x_1 \rightarrow x_3$, while the interaction of $x_2 \rightarrow x_1$ and $x_1 \rightarrow x_3$ are similar strength. This is in agreement with the simulated interaction strength.

First of all, only the valid interactions are detected by the renormalized partial directed coherence. Moreover, the influence from process $x_4 \rightarrow x_5$ and vice versa $x_5 \rightarrow x_4$ are of similar strength as the renormalized partial directed coherences take similar values. The interaction from process $x_2 \rightarrow x_3$ and $x_1 \rightarrow x_4$ are stronger than the $x_1 \rightarrow x_3$, while the interaction of $x_2 \rightarrow x_1$ and $x_1 \rightarrow x_3$ are of similar strength. This is in agreement with the simulated interactions. High coefficient values in the autoregressive model correspond to high renormalized partial directed coherence values.

3.2. Vector autoregressive process II

To complement the analysis above, a more rigorous study is performed in this section that shows that the statistics of $\hat{\lambda}_{ij}^{\circ}(\omega)$ is also suitable for $\hat{\lambda}_{ij}(\omega)$. To this aim, the five-dimensional VAR[2] process:

$$x_1(t) = 1.9x_1(t-1) - 0.999x_1(t-2) + \eta_1(t), \quad (16)$$

$$x_2(t) = 0.9x_2(t-2) - 0.2x_1(t-1) + \eta_2(t), \quad (17)$$

$$x_3(t) = -0.3x_3(t-1) + 0.4x_4(t-1) - 0.3x_5(t-2) + \eta_3(t), \quad (18)$$

$$x_4(t) = 1.3x_4(t-1) - 0.7x_4(t-2) + \eta_4(t), \quad (19)$$

$$x_5(t) = 0.7x_5(t-2) + 0.3x_1(t-1) + \eta_5(t), \quad (20)$$

has been simulated 1000 times with 3000 data points each. The investigated VAR process covers a variety of parameter values. Here the order of the fitted VAR process was 50. The 1000 realizations allow estimation of an empirical critical value for a certain significance level. Having 1000 realizations at hand the highest and lowest 25 renormalized partial directed coherence values are skipped. The interval between these two is the empirical 95% confidence interval of the average renormalized partial directed coherence. In Fig. 2 the results are displayed. The dashed black lines indicate these empirical confidence intervals. For all subplots but (2, 1), (3, 4), (3, 5), and (5, 1), where (i, j) is the subplot in the i th row and j th column, they comprise zero. This argues for the following directed interactions: $x_1 \rightarrow x_2$, $x_4 \rightarrow x_3$, $x_5 \rightarrow x_3$, and $x_1 \rightarrow x_5$, which corresponds to the simulated ones. The result of the 1001st realization

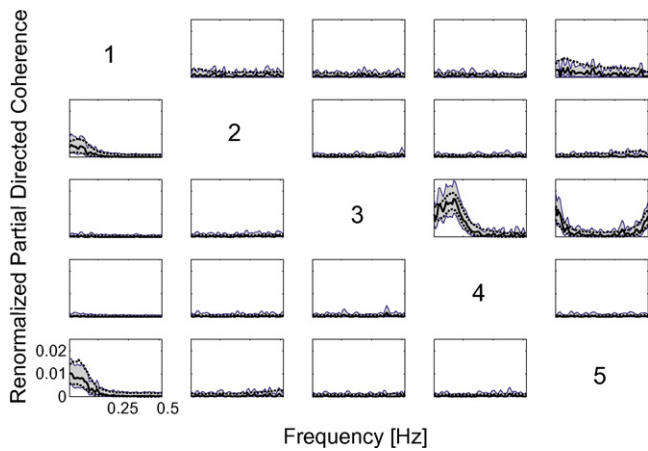


Fig. 2. Renormalized partial directed coherence (off-diagonal) for the example of the VAR[2] process. The results are sorted as a matrix, where in the i th row and the j th column the influence from process j onto process i is displayed. The black line represents the renormalized partial directed coherence values while the gray areas mark the corresponding 95% confidence intervals of one single realization. From 1000 realizations empirical confidence intervals have been derived. These are indicated by the dashed black lines. Only the valid interactions are revealed by this analysis.

is also contained in the same plot indicated by the black line and the gray areas. Thereby, the gray areas represent the confidence intervals derived above used for the plugin-estimator $\hat{\lambda}_{ij}^\circ(\omega)$ instead of $\hat{\lambda}_{ij}(\omega)$. We want to stress that they are derived from this one single realization. Analyzing these renormalized partial directed coherence values yield very similar results as the 1000 realizations. The confidence intervals comprise zero for almost all subplots but (2, 1), (3, 4), (3, 5), and (5, 1), which are the same as above. However, the confidence intervals from one single observation seem to be slightly larger than the ones obtained from the 1000 realizations. This becomes evident since the gray area usually contains the black dashed lines. Thus, the confidence intervals are shown to be reasonable and the statistics from $\hat{\lambda}_{ij}^\circ(\omega)$ suits for $\hat{\lambda}_{ij}(\omega)$.

Moreover, we substantiate that the renormalized partial directed coherence $\hat{\lambda}_{ij}^\circ(\omega)$ is χ_2^2 -distributed under the null hypothesis. To this aim, the distribution of the 1000 realizations at an arbitrarily chosen frequency of 0.08 Hz are displayed in Fig. 3 in (a) for the subplot (3, 1), in (b) for (2, 3), and in (c) for (3, 4). The vertical line indicates the 95% significance level which corresponds to a critical value of 0.002. In (a) and (b) there are hardly any values above the critical value. Indeed the significance level is conservative. In contrast in (c) where a directed influence is present the corresponding histogram is distant from the critical value indicating 100% power, i.e. the ability to detect the violation of the null hypothesis, of the proposed renormalized partial directed coherence in this setting.

To illustrate the power of the renormalized partial directed coherence to detect interactions if present, a two-dimensional autoregressive process:

$$x_1(t) = 1.7x_1(t - 1) - 0.9x_1(t - 2) + \eta_1(t), \quad (21)$$

$$x_2(t) = 0.9x_2(t - 2) - ax_1(t - 1) + \eta_2(t), \quad (22)$$

with a simulation period of 5000 data points has been analyzed. The parameter a quantifies the strength of the influence from x_1 onto x_2 while there is no causal influence in the opposite direction. The order of the fitted VAR process was again set to 50. In Fig. 4 (a) the interdependence from process x_2 onto x_1 is correctly revealed by renormalized partial directed coherence analysis for $a > 0.03$ at a frequency of 0.08 Hz, which is indicated by the fact that zero is not comprised in the gray area representing the 95% quantiles of

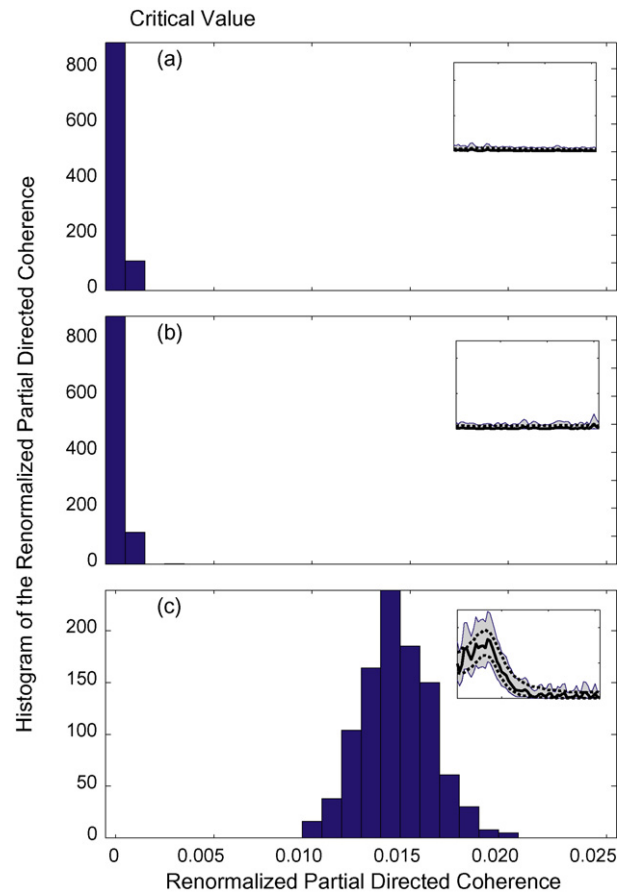


Fig. 3. Histograms of the distribution of the 1000 realizations of renormalized partial directed coherence values: (a) for subplot (3, 1), (b) for (2, 3), and (c) for (3, 4). The smaller subplots are copied from Fig. 2.

the renormalized partial directed coherence (black line). For lower parameters a the lower confidence level is compatible with zero. Thus, the direction of information transfer is correctly detected for a considerable large range of parameter values. A Granger-causal

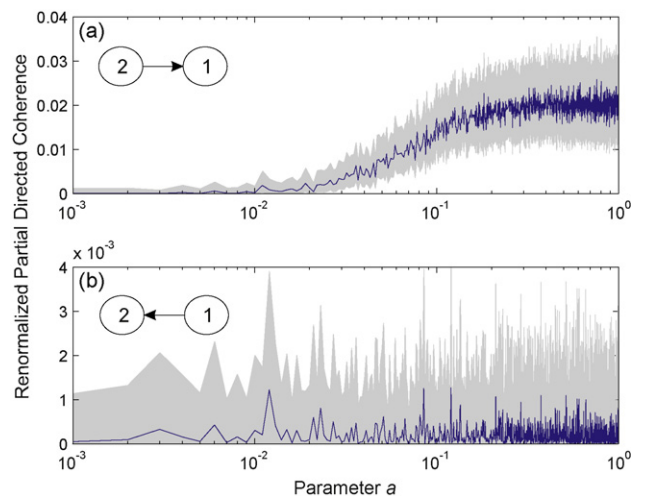


Fig. 4. Renormalized partial directed coherence for varying parameter a representing a causal influence from x_2 onto x_1 . The black line represents renormalized partial directed coherence values with its confidence band (gray area). (a) The information transfer from x_2 onto x_1 is correctly revealed for $a > 0.03$ while in (b) the renormalized partial directed coherence is always compatible with zero for the opposite direction. Please note the difference in the scale of the vertical axis by an order of a magnitude.

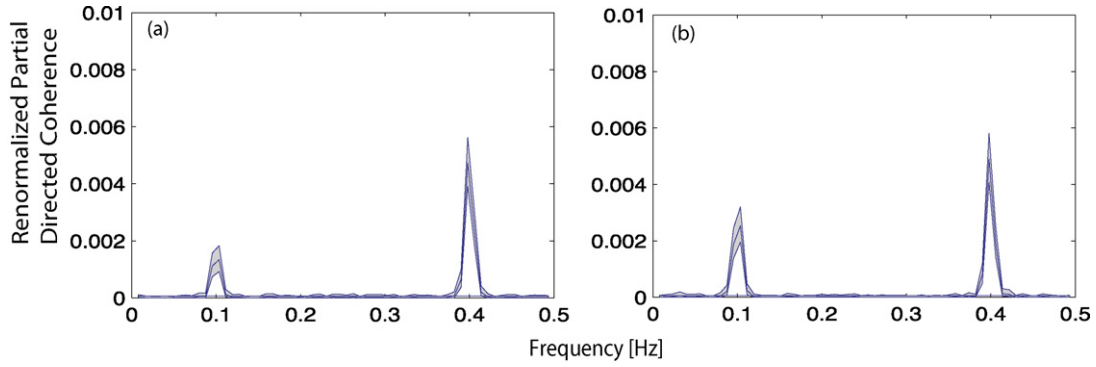


Fig. 5. Renormalized partial directed coherence. The black line represents the renormalized partial directed coherence values while the gray areas mark the corresponding 95% confidence intervals. The relative interaction strength at the two dominant frequencies of $f_1 = 0.1$ and $f_2 = 0.4$ was varied: (a) for f_1 it was 0.4 and for f_2 0.8; (b) for f_1 it was 0.6 and for f_2 0.8.

influence from x_1 onto x_2 is in accordance with the simulated system not observed (Fig. 4(b)).

To check whether renormalized partial directed coherence is able to reveal the interaction strength at different frequencies between two processes, we simulated a mixture of two autoregressive processes of order 2:

$$x_i(t) = a_i x_i(t-1) + b_i x_i(t-2) + \eta_i(t), \quad (23)$$

with

$$a_i = 2e^{-(1/\tau_i)} \cos \frac{2\pi}{T_i} \quad \text{and} \quad b_i = e^{-(2/\tau_i)}, \quad (24)$$

for $i = 1$ and 2. The parameters have been chosen to be $T_1 = 10$, $T_2 = 2.5$, and $\tau_1 = \tau_2 = 100$ resulting in the oscillation frequencies $f_1 = 0.1$ and $f_2 = 0.4$. Both processes were filtered around their oscillation frequency with a FIR filter of order 30 and normalized to unit variance. The relative strength of interaction (delay 50 data points) of these processes onto process $x_3(t)$ was varied. Observed were the processes $y_1(t) = x_1(t) + x_2(t) + 3\eta_{y_1}(t)$ and $y_2(t) = x_3(t) + 3\eta_{y_2}(t)$. The $\eta_i(t)$ are standard white noise processes. Simulated were 100,000 data points to get reliable estimates of the interaction strengths. Fitted was an autoregressive process of order 70.

In Fig. 5 the results of the renormalized partial directed coherence analysis are shown for two different relative strengths. In Fig. 5(a), the strength of the influence at the frequency $f = 0.1$ was 0.4 while the one at frequency $f_2 = 0.4$ was 0.8. In Fig. 5(b), the strength of the influence at the frequency $f_1 = 0.1$ was 0.6 while the one at frequency $f_2 = 0.4$ was 0.8. This result illustrates that renormalized partial directed coherence is able to measure the interaction strength between two processes at different frequencies. We mention that similar to the results shown in Fig. 4 the relation between the renormalized partial directed coherence value and the interaction strength seems to be non-linear. Additionally, the renormalized partial directed coherence values are compatible between (a) and (b) at $f = 0.4$, which has to be the case as both strengths of interaction have been simulated with 0.8.

The opposite direction from process y_2 on y_1 was not detected by renormalized partial directed coherence which is again in accordance with the simulation. The results are not shown.

3.3. Vector autoregressive process III

As a third example the following five-dimensional VAR[2] process.

$$x_1(t) = 0.9x_1(t-1) - 0.3x_1(t-2) + \eta_1(t), \quad (25)$$

$$x_2(t) = 0.6x_2(t-1) + 0.2x_4(t-2) + \eta_2(t), \quad (26)$$

$$x_3(t) = 0.5x_3(t-1) + 0.4x_2(t-2) + 0.4x_4(t-1) + 0.2x_5(t-2) + \eta_3(t), \quad (27)$$

$$x_4(t) = 1.2x_4(t-1) - 0.4x_4(t-2) + \eta_4(t), \quad (28)$$

$$x_5(t) = 0.3x_5(t-1) + 0.3x_5(t-2) + 0.2x_3(t-1) + 0.3x_4(t-1) + 0.2x_1(t-2) + 0.3x_2(t-2) + \eta_5(t), \quad (29)$$

is used. This example is utilized to show that the renormalized partial directed coherence does not measure the strength of influences relative to a given signal source. Renormalized partial directed coherence should not be influenced by the number of other series that are influenced by the source process.

As shown in Fig. 6 (a), the renormalized partial directed coherence again correctly reproduces the interaction structure realized by the simulated model system. Only those $\hat{\lambda}_{ij}^\circ(\omega)$ that correspond to non-zero coefficients in the VAR[2] process above are significantly different from zero. In Fig. 6(b) the result is shown, when the above VAR[2] is simplified to

$$x_1(t) = 0.9x_1(t-1) - 0.3x_1(t-2) + \eta_1(t), \quad (30)$$

$$x_2(t) = 0.6x_2(t-1) + \eta_2(t), \quad (31)$$

$$x_3(t) = 0.5x_3(t-1) + 0.4x_4(t-1) + \eta_3(t), \quad (32)$$

$$x_4(t) = 1.2x_4(t-1) - 0.4x_4(t-2) + \eta_4(t), \quad (33)$$

$$x_5(t) = 0.3x_5(t-1) + 0.3x_5(t-2) + \eta_5(t). \quad (34)$$

In other words, all interactions are absent but the interaction from process x_4 to x_3 , which is kept constant. Since the absolute value of $\hat{\lambda}_{34}^\circ(\omega)$ remains unchanged with respect to the confidence intervals, we have illustrated that renormalized partial directed coherence does not measure the strength of interactions relative to a given signal source.

To summarize the above results, renormalized partial directed coherence $\hat{\lambda}_{ij}^\circ(\omega)$ has been assessed by means of different model systems. It has been shown to be a powerful technique to infer the interaction structure in these systems. The rigorous assessment has moreover demonstrated that the technique is slightly conservative but that the power is sufficiently high to be able to detect interactions if present and that the derived statistics that is strictly only valid for $\hat{\lambda}_{ij}^\circ(\omega)$ can be readily applied. Additionally, fitting models of order 50, which is more than 10 times higher than the true process order, does not hamper the applicability of the renormalized partial directed coherence. Thus, we can conclude similar to ordinary partial directed coherence that overfitting the data favorable compared to underfitting the process since the latter would result in false positive conclusions about the

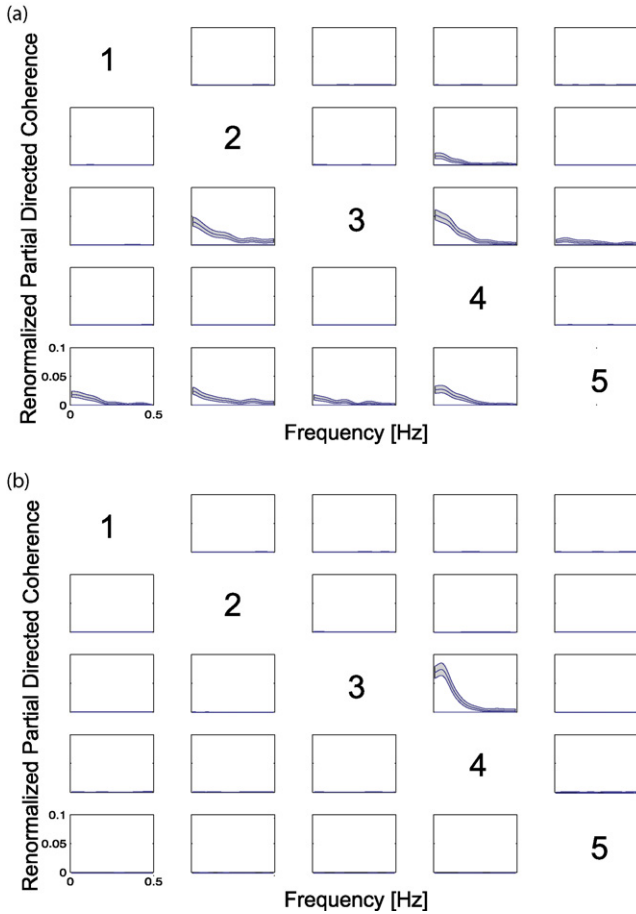


Fig. 6. Renormalized partial directed coherence (off-diagonal) for the example of the VAR[2] process of section “vector autoregressive process III”. The results are sorted as a matrix: in the i th row and the j th column the influence from process j onto process i is displayed. The black line represents the renormalized partial directed coherence values while the gray areas mark the corresponding 95% confidence intervals. (a) The entire system is correctly revealed by the renormalized partial directed coherence. (b) Only the directed influence between process x_4 and x_3 remains constant, all the others are zero.

coupling. We like to stress that prior to any application we recommend testing renormalized partial directed coherence tailored to the problem.

3.4. Coupled van-der-Pol oscillators

As demonstrated above, renormalized partial directed coherence analysis is able to detect the network structure underlying linear vector autoregressive processes, for which it has been developed. To demonstrate its wide-spread applicability we applied it to a system of coupled stochastic van-der Pol oscillators:

$$\ddot{x}_i = \mu(1 - x_i^2)\dot{x}_i + \omega_i^2 x_i + \sigma_i \eta_i + \sum_{j \neq i} \epsilon_{ij}(x_j - x_i) \quad (35)$$

for $i = 1, \dots, 4$. The non-linearity parameter was chosen to be $\mu = 5$ for all oscillators, the standard deviation of the Gaussian white noise η_i was $\sigma_i = 1.5$. The frequency of the four oscillators was slightly detuned around $\omega = 2\pi f = 1.5$ Hz by setting $\omega_1 = 1.5$ Hz, $\omega_2 = 1.53$ Hz, $\omega_3 = 1.48$ Hz, and $\omega_4 = 1.44$ Hz. The coupling scheme ensures that oscillators 1 and 2 are mutually coupled while the coupling from oscillator 1 onto 4 and from 3 onto 1 was unidirectional. The parameters were $\epsilon_{12} = \epsilon_{21} = 0.4$, $\epsilon_{13} = 0.4$, and $\epsilon_{42} = 0.4$. In Fig. 7 the results of renormalized partial directed coherence analysis

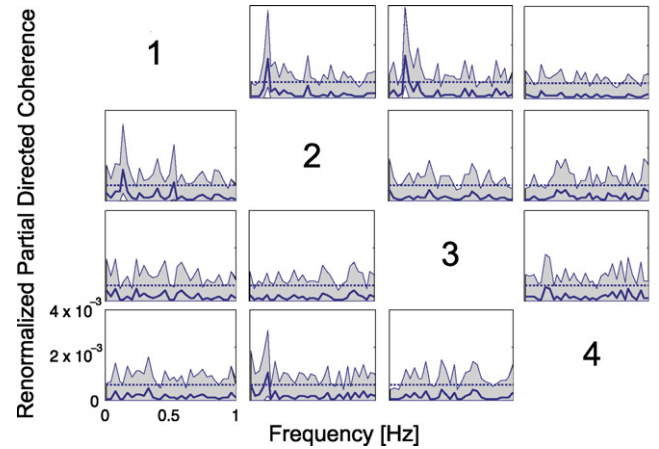


Fig. 7. Results of the renormalized partial directed coherence analysis for a network of four coupled van-der-Pol oscillators. The coupling is bidirectional between oscillators 1 and 2 and unidirectional from oscillator 2 to oscillator 4 and from oscillator 3 to oscillator 1. The dashed horizontal line marks the 5% significance level, while the gray area represents the 95% confidence intervals.

for 10,000 data points for each oscillator and a model order $p = 200$ are depicted. The dotted horizontal line marks the 5%-significance level, while the gray area represents the 95% confidence intervals. At the oscillation frequency of approximately 0.2 Hz only those renormalized partial directed coherence values are significant that correspond to the true interaction structure.

To further substantiate this finding we varied the coupling between two van-der-Pol oscillators. As it is visible from Fig. 8 the renormalized partial directed coherence values evaluated at the oscillation frequency increase for increasing coupling between the oscillators. Thus, renormalized partial directed coherence does not only detect the true interaction structure but provides additionally a measure for the strength of the interaction also in non-linear stochastic systems.

3.5. Coupled Rössler oscillators

To demonstrate that renormalized partial directed coherence is capable in providing the actual interaction structure also for chaotic

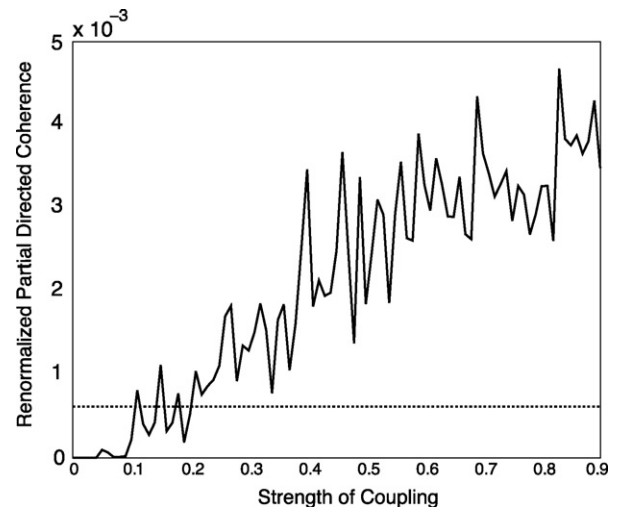


Fig. 8. Coupled van-der-Pol oscillators. Renormalized partial directed coherence for various coupling strengths ϵ_{12} . The dashed horizontal line marks the 5% significance level.

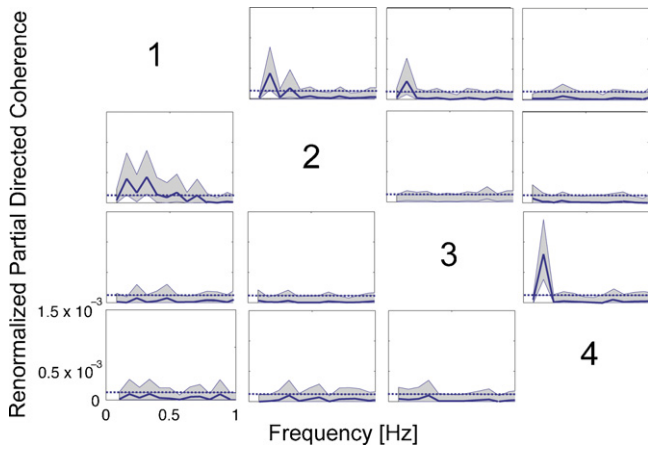


Fig. 9. Results of the renormalized partial directed coherence analysis for a network coupled Rössler oscillators. The coupling is bidirectional between oscillators 1 and 2 and unidirectional from oscillator 2 to oscillator 4 and from oscillator 4 to oscillator 3. The dashed horizontal line marks the 5% significance level, while the gray area represents the 95% confidence intervals.

systems, four coupled stochastic Rössler oscillators

$$\dot{\xi}_j = \begin{pmatrix} \dot{X}_j \\ \dot{Y}_j \\ \dot{Z}_j \end{pmatrix} = \begin{pmatrix} -\omega_j Y_j - Z_j + \left[\sum_{i,i \neq j} \varepsilon_{j,i} (X_i - X_j) \right] + \sigma_j \eta_j \\ \omega_j X_j + a Y_j \\ b + (X_j - c) Z_j \end{pmatrix}, \quad (36)$$

$i, j = 1, \dots, 4$

have been simulated with 50,000 data points with a sampling rate of 10 Hz. The integration step was 0.004. The parameters are set to $a = 0.15$, $b = 0.2$, $c = 10$, $\omega_1 = 2\pi f_1 = 1.01$, $\omega_2 = 2\pi f_2 = 0.99$, $\omega_3 = 2\pi f_3 = 0.97$, and $\omega_4 = 2\pi f_4 = 1.03$ ensuring a chaotic behavior in the deterministic case. For the noise term $\sigma_j \eta_j$ a standard deviation of $\sigma_j = 1.0$ is chosen and η_j is standard Gaussian distributed. The bidirectional coupling $\varepsilon_{12} = \varepsilon_{21} = 0.04$ between oscillator ξ_1 and oscillator ξ_2 and the unidirectional coupling between oscillators ξ_3 and oscillator ξ_1 , $\varepsilon_{31} = 0.04$, and between oscillators ξ_4 and oscillator ξ_3 , $\varepsilon_{34} = 0.04$, corresponds to phase synchronization between the oscillators.

The X-components of the individual oscillators enter the renormalized partial directed coherence analysis with a model order $p = 250$. From the results in Fig. 9 the true interaction structure can be reproduced. This demonstrates that renormalized partial directed coherence is capable in revealing the actual interaction structure also for non-linear chaotic systems.

4. Application to Parkinsonian tremor

Indications for the pathophysiological basis of Parkinsonian tremor, a common neurological disease, have been found from animal experiments and some human studies (Hellwig et al., 2000). Parkinsonian tremor manifests itself mainly in the upper limbs, usually when the hands are in a relaxed position. Parkinsonian tremor is a unilateral form of tremor, i.e. in general the trembling occurs on one side. The trembling frequency of the hand is 4–10 Hz. To elucidate the tremor generating mechanisms in Parkinsonian tremor, relationships between the brain and trembling muscles are of particular interest. Tremor correlated cortical activity has been observed by coherence analysis of simultaneously recorded electroencephalography and electromyography (Hellwig et al., 2000). Within that study it was not possible to differentiate whether the cortex imposes its oscillatory activity on the muscles via the corti-

cospinal tract or whether the muscle activity is just reflected in the cortex via proprioceptive afferences. No consistent results could be detected by analyzing the phase spectra. Moreover, interactions at the tremor frequency and at the first higher harmonic have been detected. It stands to elucidate which of the two frequencies is of particular importance for Parkinsonian tremor. Therefore, to get deeper insights into tremor generation, partial directed coherence analysis and renormalized partial directed coherence analysis is applied to data recorded from patients suffering from Parkinsonian tremor.

For one illustrative patient with Parkinsonian tremor, the EMG from the right wrist extensor as well as the EEG recorded over the left sensorimotor cortex are analyzed. Unilateral postural tremor was recorded for 300 s using a sampling rate of 1000 Hz. EEG data were band-pass filtered between 0.5 Hz and 200 Hz. To avoid movement artifacts, EMG data were band-pass filtered between 30 Hz and 200 Hz and rectified afterwards. Since the raw EMG is essentially modulated noise, taking the absolute value after subtracting the mean, which is referred to as rectification, is mandatory. It ensures to get the modulation function of the noise which constitutes the physiologically meaningful signal. The filters applied are to avoid movement artifacts and to avoid aliasing and are therefore essential for a reasonable analysis of the data. The hardware filter itself has been proven not to introduce unwanted delays between the time series.

In Fig. 10 a, results of the partial directed coherence analysis for the EMG and the EEG channel are shown. On the diagonal the spectra of the processes are given. The tremor frequency indicated by the sharp peak in the right EMG-spectrum is almost 5 Hz. Significant partial directed coherences at the corresponding tremor frequency and its higher harmonics are detected for the direction from the right EMG to the left, contralateral EEG, and vice versa.

The partial directed coherence indicating a causal influence from the right EMG to the left EEG is much higher than the partial directed coherence indicating a causal influence from the left EEG to the right EMG (Fig. 10). Moreover the influence at the double tremor frequency appears to be almost as strong as the one at the tremor frequency. The significance level increases at the tremor frequency for the influence from the EMG to the EEG; this might already indicate that the influences are not of equal importance. This, however, cannot be investigated using partial directed coherence.

In Fig. 10 b, the results of the renormalized partial directed coherence are displayed in the same way as for the ordinary partial directed coherence. It is now visible that the influence at the first higher harmonic frequency from the EMG onto the EEG is higher than the one at the tremor frequency. The afferent influence is more pronounced at the double tremor frequency than at the tremor frequency itself even though both contribute. Interactions at the double tremor frequency seem to be important for the afferent interactions between cortical signals and the muscle activity.

The results found for directed influences from the cortex to the muscles and in the opposite direction are comparable under the assumption that the signal-to-noise ratio is similar for both processes. This is hardly expected in the case of EEG and EMG. While the EMG represents a signal with very high signal-to-noise ratio the EEG is expected to be contaminated with a lot of noise. Thus, we can only state that there is influence from the cortex onto the muscles.

In summary, since causal influences from the EEG to the corresponding contralateral EMG are present, participation of the motor cortex in tremor generation is strongly indicated. Moreover, there is also a significant partial directed coherence from the EMG to the contralateral EEG at the tremor frequency. This corresponds

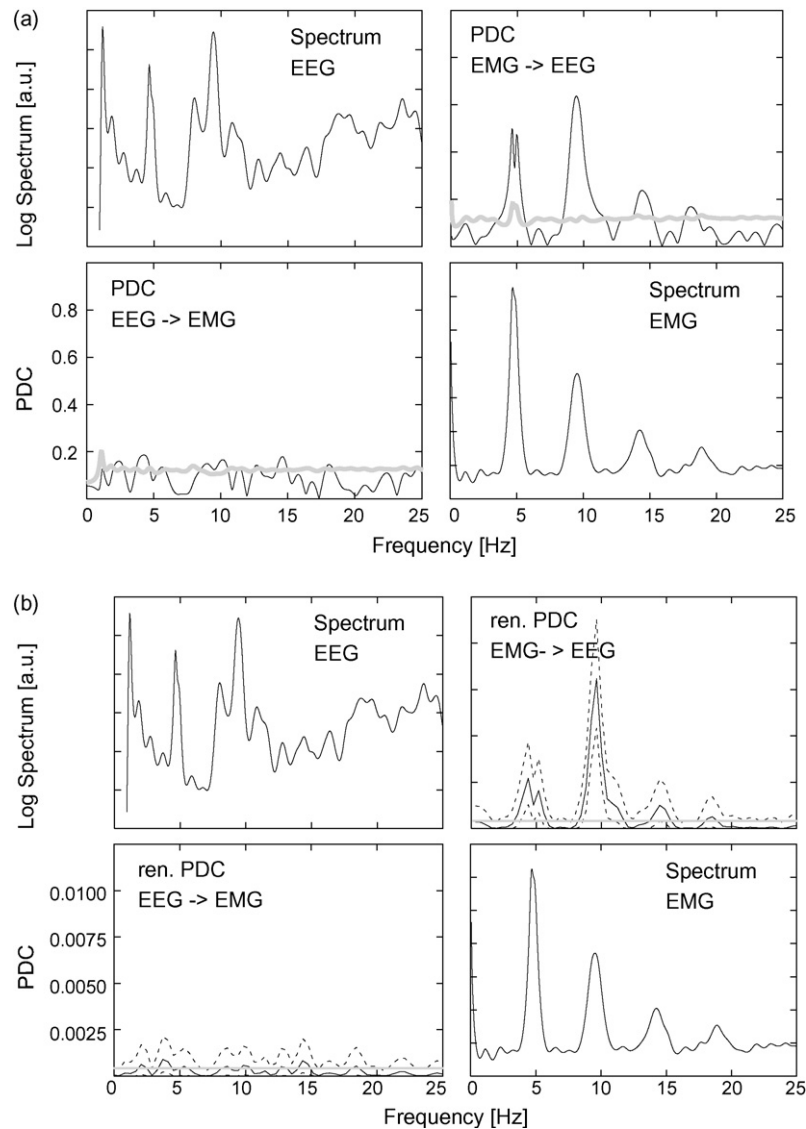


Fig. 10. Partial directed coherence (a) and renormalized partial directed coherence (b) for a representative example of a patient suffering from Parkinsonian tremor. On the diagonals the spectra of the electroencephalogram and electromyogram are shown. The off-diagonal elements show the partial directed coherence and the renormalized partial directed coherences, respectively. Directed influences in both directions are present. However, only the renormalized version of partial directed coherence is able to decide that the directed influence from the EMG onto the EEG at the tremor frequency is statistically significantly lower than at the first higher harmonic.

to a feedback from the muscles to the somatosensory cortex. Especially for this feedback the influence at the first higher harmonic frequency seems to be very important for Parkinson tremor. Physiological consequences from this result should be based on the analysis of more patients which is beyond the scope of this manuscript but currently under investigation.

5. Conclusion

Partial directed coherence is a powerful analysis technique to detect causal influences in multivariate stochastic systems with respect to Granger-causality. However, partial directed coherence suffers from some conceptual problems that manifest themselves in an arbitrary and disadvantageous normalization. We presented a way out of this dilemma by suggesting a different normalization strategy. For this renormalized partial directed coherence calculation of the statistical properties is also possible. Moreover, it was possible to derive confidence intervals that hold under the null hypothesis of absent coupling but also under the alternative hypothesis.

The performance of the proposed renormalized partial directed coherence, its confidence intervals, and significance level has been shown by means of a linear and non-linear, including chaotic, stochastic model system. We have presented an exemplary application to EEG and EMG data from a patient suffering from Parkinsonian tremor. Using partial directed coherence and especially renormalized partial directed coherence in combination with the confidence intervals and the significance level allows to detect causal influences between EEG and EMG recordings in Parkinsonian tremor and provides thus closer insights into the tremor generating mechanisms. A distinction of the strength of the directed influence between the tremor frequency and its higher harmonic became possible.

Acknowledgements

Special thank go to Bernhard Hellwig and Professor Carl Hermann Lücking who provided us not only with the tremor data but also with knowledge about the neurophysiology of Parkinsonian tremor. Moreover the authors like to thank John T. Kent for

providing us with the program for computing confidence intervals for the noncentrality parameter of noncentral χ^2 -distributions.

This work was supported by the German Science Foundation (Ti315/4-2) and by the German Federal Ministry of Education and Research (BMBF grant 01GQ0420). This work was supported by the Excellence Initiative of the German Federal and State Governments.

References

- Baccala L, Sameshima K. Partial directed coherence: a new concept in neural structure determination. *Biol Cybern* 2001;84:463–74.
- Bloomfield P. *Fourier analysis of time series: an introduction*. New York: John Wiley & Sons; 1976.
- Dahlhaus R, Eichler M, Sandkühler J. Identification of synaptic connections in neural ensembles by graphical models. *J Neurosci Methods* 1997;77:93–107.
- Eichler M, Dahlhaus R, Sandkühler J. Partial correlation analysis for the identification of synaptic connections. *Biol Cybern* 2003;89:289–302.
- Eichler M. On the evaluation of information flow in multivariate systems based on the directed transfer function. *Biol Cybern* 2006;94:469–82.
- Granger J. Investigating causal relations by econometric models and cross-spectral methods. *Econometrica* 1969;37:424–38.
- Grosse P, Cassidy M, Brown P. EEG–EMG, MEG–EMG and EMG–EMG frequency analysis: physiological principals and clinical applications. *Clin Neurophysiol* 2002;113:1523–31.
- Hellwig B, Häußler S, Lauk M, Köster B, Guschlbauer B, Kristeva-Feige R. Tremor-correlated cortical activity detected by electroencephalography. *Electroencephalogr Clin Neurophysiol* 2000;111:806–9.
- Hellwig B, Häußler S, Schelter B, Lauk M, Guschlbauer B, Timmer J. Tremor correlated cortical activity in essential tremor. *Lancet* 2001;357:519–23.
- Hellwig B, Schelter B, Guschlbauer B, Timmer J, Lücking CH. Dynamic synchronisation of central oscillators in essential tremor. *Clin Neurophysiol* 2003;114:1462–7.
- Hesse W, Möller E, Arnold M, Schack B. The use of time-variant EEG Granger-causality for inspecting directed interdependencies of neural assemblies. *J Neurosci Methods* 2003;124:27–44.
- Johnson NL, Kotz S, Balakrishnan N. *Continuous univariate distributions*, vol. 2. Wiley; 1995.
- Kamiński MJ, Blinowska KJ. A new method of the description of the information flow in the brain structures. *Biol Cybern* 1991;65:203–10.
- Kamiński MJ, Ding M, Truccolo WA, Bressler SL. Evaluating causal relations in neural systems: Granger causality, directed transfer function and statistical assessment of significance. *Biol Cybern* 2001;85:145–57.
- Kent J, Hainsworth T. Confidence intervals for the noncentral chi-squared distribution. *J Stat Plan Infer* 1995;46:147–59.
- Lütkepohl H. *Introduction to multiple time series analysis*. Springer; 1993.
- Rosenblum M, Pikovsky A. Detecting direction of coupling in interacting oscillators. *Phys Rev E* 2001;64:045202.
- Sameshima K, Baccala L. Using partial directed coherence to describe neuronal ensemble interactions. *J Neurosci Methods* 1999;94:93–103.
- Schelter B, Winterhalder M, Eichler M, Peifer M, Hellwig B, Guschlbauer B. Testing for directed influences among neural signals using partial directed coherence. *J Neurosci Methods* 2006;152:210–9.
- Smirnov DA, Bezruchko BP. Estimation of interaction strength and direction from short and noisy time series. *Phys Rev E* 2003;68:046209.
- Tass P, Rosenblum MG, Weule J, Kurths J, Pikovsky A, Volkmann J. Detection of $n:m$ phase locking from noisy data: application to magnetoencephalography. *Phys Rev Lett* 1998;81:3291–5.
- Timmer J, Lauk M, Pfleger W, Deuschl G. Cross-spectral analysis of physiological tremor and muscle activity. I. Theory and application to unsynchronized EMG. *Biol Cybern* 1998;78:349–57.
- Volkmann J, Joliot M, Mogilner A, Ioannides A, Lado F, Fazzini E. Central motor loop oscillations in Parkinsonian resting tremor revealed by magnetoencephalography. *Neurology* 1996;46:1359–70.
- Winterhalder M, Schelter B, Hesse W, Schwab K, Leistriz L, Klan D. Comparison of linear signal processing techniques to infer directed interactions in multivariate neural systems. *Sig Proc* 2005;85:2137–60.